PAPER

An infrared study of solid glycine in environments of astrophysical relevance

Belén Maté,* Yamilet Rodriguez-Lazcano, Óscar Gálvez, Isabel Tanarro and Rafael Escribano

The conversion from neutral to zwitterionic glycine is studied using infrared spectroscopy from the point of view of the interactions of this molecule with polar (water) and non-polar (CO_2, CH_4) surroundings. Such environments could be found on astronomical or astrophysical matter. The samples are prepared by vapour-deposition on a cold substrate (25 K), and then heated up to sublimation temperatures of the co-deposited species. At 25 K, the neutral species is favoured over the zwitterionic form in non-polar environments, whereas for pure glycine, or in glycine/water mixtures, the dominant species is the latter. The conversion is easily followed by the weakening of two infrared bands in the mid-IR region, associated to the neutral structure. Theoretical calculations are performed on crystalline glycine and on molecular glycine, both isolated and surrounded by water. Spectra predicted from these calculations are in reasonable agreement with the experimental spectra, and provide a basis to the assignments. Different spectral features are suggested as probes for the presence of glycine in astrophysical media, depending on its form (neutral or zwitterionic), their temperature and composition.

Introduction

The identification of interstellar organic molecules is a subject of great interest, as they may provide important insights into the history of the solar system and the origin of life on Earth. Amino acids have been found in Solar System bodies and meteorites,[1–3] and in particular, cometary grains collected by the NASA Stardust mission[4,5] have been shown to contain glycine,[6] (NH_2CH_2COOH), the simplest of the amino acids and the most vastly studied and searched. Glycine was also found in the analysis of the Almahata Sitta Meteorite,[7] and although the authors could not discard some terrestrial contamination, the racemic composition of alanine in the meteorite indicated an alien origin of these amino acids. However, this subject is controversial to a high degree; see for instance the recent publication claiming fossils in meteorites[8] and the heated discussion that it is generating.

In the laboratory, it has been demonstrated that glycine can be formed from ultraviolet irradiation of icy interstellar analogs,[9–14] in the midst of a complex assortment of chemical species generated in the reactions induced by the irradiation. Although recent works have extended the spectroscopic range of study of amino acids even up to the vacuum ultraviolet,[15] infrared spectroscopy is a frequently used tool to study laboratory generated amino acids,[16] as well as to derive much

of the available information on astrophysical ices, either from space or terrestrial observatories. The extension of laboratory infrared studies of amino acid molecules in different icy environments seems therefore of evident usefulness.

Glycine has the particularity that in water solution or in crystalline phases (α, β or γ) it adopts a zwitterionic form ($^{+}NH_3CH_2COO^{-}$), whereas in the gas phase or in low-temperature inert matrices it exists in its neutral form.[17–19] The disposition of the amino and the carboxyl groups in the neutral species gives rise to three possible molecular structures that were early investigated by matrix-isolation by Stepanian *et al.*[18] These authors also applied theoretical techniques to study their relative stabilities, a subject dealt later by Pacios *et al.*[20] Acid and alkaline forms of glycine, with Cl^- and Na^+, respectively, were also studied by Rosado *et al.*[21] The association of glycine with water has given rise to recent studies of different types, using matrix-isolation Fourier transform infrared (FTIR) spectroscopy of glycine–water complexes,[22] or focussed on the adsorption of glycine molecules on ice surfaces,[23,24] and also of a theoretical nature, either by density functional theory (DFT) methods,[22] or using molecular dynamics.[25] Closer to the interest of this work is the thorough investigation by Gómez-Zavaglia and Fausto[26] of the existence and interconversion of the neutral and zwitterionic forms for glycine and two methyl derivatives, using FTIR spectroscopy. They generated pure glycine solids by depositing neutral glycine vapour, sublimated in an oven at 87 or 64 °C, on a very cold substrate (9 K), observing the neutral form of glycine

Instituto de Estructura de la Materia, IEM-CSIC, Serrano 121-123, 28006 Madrid, Spain. E-mail: belen.mate@csic.es

12268 | *Phys. Chem. Chem. Phys.*, 2011, **13**, 12268–12276

This journal is © the Owner Societies 2011

in the solid state. They also noted that the proportion of neutral and zwitterionic forms in the solid depends on both the generation conditions of the vapour and the temperature of the deposition substrate. Upon annealing the amorphous neutral form irreversibly transforms into the zwitterionic one. The transformation can be followed by the evolving IR spectrum, which in these conditions is similar to the spectrum of crystalline α-glycine.

Whereas glycine has thus received considerable attention both as a solid and in water solution, mixed species with other components, like CO_2 or CH_4, have not been studied yet, as far as we know. In astronomical or astrophysical media, such mixtures can be expected to occur, and this provides one of the reasons to undertake the present investigation.

We have generated low temperature solid binary mixtures (from 25 K to 200 K) of glycine with water, carbon dioxide or methane containing about 0.5% of glycine, a proportion that is still probably high for astrophysical objects, but could be taken as a model for laboratory work. The mixed ice films have been studied by Fourier Transform Infrared spectroscopy. Our research is complemented by theoretical calculations and predictions of the IR spectra of solid crystalline glycine and of the gas phase glycine monomer and dimer.

Experimental and computational methods

Experimental setup

The experimental setup was described in detail elsewhere.[27,28] In brief, it consists of a high vacuum chamber provided with a closed cycle helium cryostat, with an infrared transparent Si substrate in contact with the cryostat cold finger. The finger can be cooled down to 14 K, although we have chosen 25 K for the present experiments. The residual pressure of the chamber at room temperature is 5×10^{-8} mbar. Through adequate windows, the system is coupled to a Bruker Vertex70 FTIR spectrometer to work in transmission configuration. The main difference to our previous setup is the present capability of rotating the cryostat under vacuum, which has been used as described below.

Glycine salt was purchased from Sigma-Aldrich (purity $\geq 99.0\%$). Low temperature solid layers were prepared by deposition of its sublimated vapour on the cold Si substrate. To evaporate the glycine a specifically designed sublimation mini-oven located inside the vacuum chamber was constructed. It consists of a copper crucible provided with a 50 W halogen lamp for heating and a chromel–alumel (tipe K) thermocouple for temperature measurements. The oven temperature is regulated by means of a proportional-integral-derivative (PID) controller. While the set-point temperature was being gained the deposition substrate was maintained tangential to the mini-oven flow. In this position the substrate holder intercepts the glycine flow, an effect that was confirmed by recording IR spectra during the oven heating process (see the scheme in Fig. 1). When the oven reached the working temperature, usually after 30 minutes of operation, the substrate was rotated and placed perpendicular to the glycine flow, and the oven was translated to position its exit hole, of 4 mm diameter, at 10 mm from the cold substrate. To finish the deposit the heating lamp was switched off and the
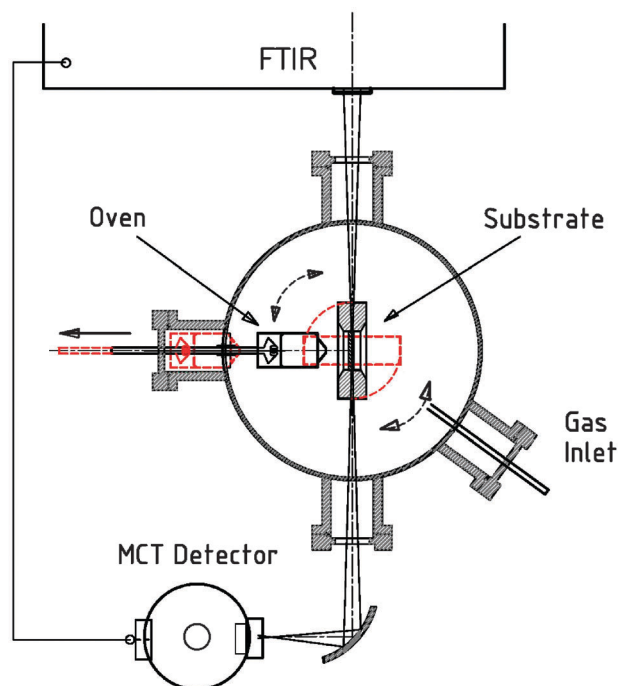

Fig. 1 Schematic representation of the cryostat, including the oven set-up.

oven was moved back to a place in contact with a copper block that accelerated its cooling.

The oven working temperature was selected to yield a high proportion of neutral glycine at 25 K. According to Gómez-Zavaglia and Fausto[26] the neutral to zwitterionic ratio in the deposit decreases with increasing oven temperature. After the initial study on the oven temperature dependence of the deposited samples described in the following section, we fixed the oven temperature at 105 °C for the rest of the experiments described in this work (Oven temperatures are indicated in Centigrade to keep a closer reference to the actual measuring employed and to avoid confusion with cryostat temperatures, expressed in Kelvin as customary). Mixed layers of glycine and the other components were prepared by introducing water vapour, CO_2 or CH_4 through an independent inlet to backfill the chamber to a controlled pressure of about 1×10^{-5} mbar at the same time that the glycine flow was being admitted. In this way a mixed glycine/ice layer was formed on one side of the substrate and a pure H_2O, CO_2 or CH_4 ice layer on the other side. In all the spectra discussed in this work the contribution of the pure species was removed by subtracting a properly scaled spectrum of the appropriate species recorded under the same experimental conditions. All spectra were recorded at 2 cm^{-1} resolution. The temperature evolution of the different spectra was followed by heating the solid deposits generated at 25 K with a 5 K min^{-1} ramp up to 200 K.

Column densities of water, CO_2 and CH_4 in the ice mixtures were calculated via the Lambert–Beer relation, using the integrated values of the infrared absorption bands and the corresponding integrated absorption coefficients, A. The bands chosen for this purpose were the ν_1 band of water around 3.1 μm (3200 cm^{-1}), the ν_3 band of CO_2 at $\sim$4.3 μm (2340 cm^{-1}), and the ν_4 band of CH_4 at $\sim$7.7 μm (1300 cm^{-1}).

Reference values were taken from ref. 29 for water, from ref. 30 for CO_2, and from ref. 31 for CH_4. We used $A = 1.9 \times 10^{-16}$ cm molecule^{-1} for water, $A = 7.1 \times 10^{-17}$ cm molecule^{-1} for CO_2, and $A = 8.085 \times 10^{-18}$ cm molecule^{-1} for pure CH_4 ice (corrected assuming a CH_4 density of 0.47 g cm^{-3} as described by Herrero et al.[32]). To determine glycine column densities we were faced with the problem of lacking experimental information on the integrated absorption coefficient of the glycine bands. We were then forced to use our calculated values for solid α-glycine. The calculated integrated band strength summing all infrared bands in the 2000–800 cm^{-1} spectral region was 1.6×10^{-15} cm molecule^{-1}. The measured integral of the spectra of glycine deposits in the same spectral region, obtained after heating our samples to 200 K, was then compared with the calculated magnitude.

The fraction of the neutral form in pure glycine samples was estimated by the 1600 cm^{-1} zwitterionic band intensity ratio between measurements at 200 K, where no neutral species remain, and those taken at 25 K. This procedure assumes that the absorption coefficient of this band does not change with temperature. In the three mixtures studied the relative intensities of the different bands of the spectra were compared with those of the pure glycine deposit in order to estimate the neutral/zwitterion fraction.

Computational methods

We have applied theoretical methods to study glycine as a solid and as an isolated molecule. For the first type, we have used the CASTEP package,[33] a program based on a density functional theory (DFT) plane-wave pseudo-potential method that is specifically designed to calculate different properties of solids, like geometry optimization and prediction of infrared spectra. In order to choose an optimum parameter set to simulate crystalline α-glycine, we have tested several correlation-exchange functionals using different parameterizations: PBE[34] and PW91[35] gradient-corrected functionals (GGA), and non-local potentials as PBE0[36] and B3LYP.[37] Dispersion corrections in two different schemes (Tkatchenko and Scheffler[38] and Grimme[39]) have also been included in the gradient correction functionals. PBE and PW91 simulations gave considerably shorter hydrogen bond distances in the optimized structure than the experimental value, around 15–20%, but the results turned out to be much more accurate when dispersion corrections were included. From these tests it follows that all methods (PBE, PW91, B3LYP, PBE0), when dispersion corrections are taken into account, give similar geometry values of the α-glycine crystal. Moreover, a similar conclusion was found regarding the IR spectrum for those cases when it was calculated, namely PBE and PW91. Consequently, we will present our results for just the PBE functional, including dispersion correction in the Tkatchenko and Scheffler[38] scheme. Convergence criteria of 1.0×10^{-5} eV atom^{-1}, 0.03 eV Å^{-1}, 0.001 Å and 0.05 GPa for energy, maximum force, maximum displacement and maximum stress, respectively, were selected. Norm-conserving pseudo-potentials with a plane wave energy cutoff of 750 eV were also used. The calculations were performed in a k-point grid of the entire Brillouin zone generated using a k-point separation of 0.07 Å^{-1}.

On the other hand, we used the Gaussian 03 suite[40] to study the isolated glycine molecule, its dimer, and glycine in a water environment. We chose a moderately high level of theory, namely B3LYP/aug-cc-pvTZ, which afforded predicting the vibrational spectra with a reasonable level of accuracy.[20] To compute the glycine monomer in a water environment, we did the calculations in a polarizable continuum model (PCM) using the default parameterization included in the Gaussian code.

Results and discussion

Pure glycine solid films

The temperature of the sublimation oven affects the proportion of neutral to zwitterionic form on the glycine deposit at low temperature. It has been proposed that the transformation from the neutral to the zwitterionic form occurs in the solid phase and depends on the energy that the molecules have previously to their deposition on a substrate held at low temperatures.[26]

In Fig. 2a we present spectra of pure glycine deposits obtained changing the temperature of the oven and maintaining the substrate at 25 K. Obviously the number of molecules evaporated, and hence the number of molecules in the sample increases with temperature. Therefore, to facilitate the
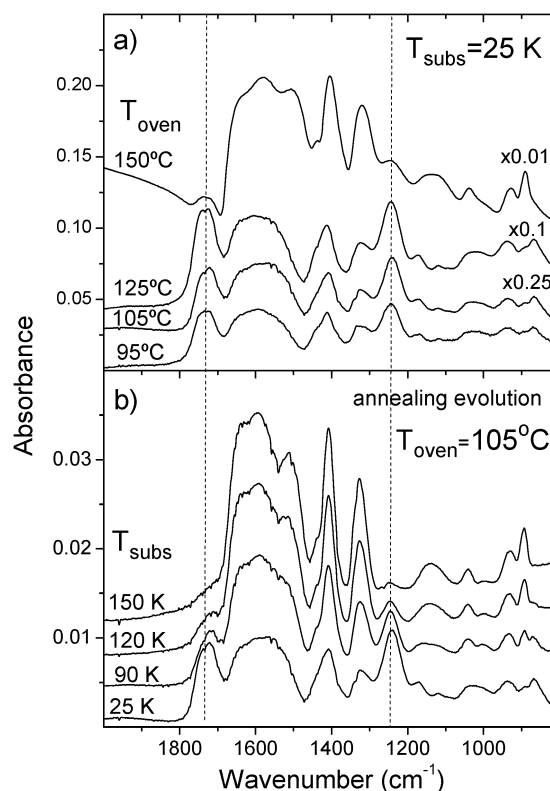

Fig. 2 (a) Spectra of glycine layers vapour-deposited at 25 K using different sublimation oven temperatures, indicated in the figure. (b) Spectra of a glycine layer generated at T_{oven} = 105 °C, vapour-deposited at T_{subs} = 25 K, and warmed to the indicated substrate temperatures. In both cases, the evolution of the neutral/zwitterionic ratio in the sample can be followed by changes on the main neutral glycine bands, marked by dashed vertical lines. Spectra are offset in the absorbance scale for clarity.

comparison, the three upper spectra in Fig. 2a corresponding to oven temperatures of 150 °C, 125 °C and 105 °C have been scaled down in intensity by factors of 0.01, 0.1 and 0.25, respectively. The two strongest bands associated to neutral glycine in the spectral range represented in Fig. 2 appear at 1730 cm^{-1} and 1240 cm^{-1} (marked with dashed lines in the figure), whereas the zwitterionic species is the main component, but not necessarily the only one, of the other bands in this zone. When the oven temperature is between 95 °C and 125 °C a nearly constant neutral to zwitterionic ratio is observed in the deposit. However, at 150 °C, the bands of the neutral species appear considerably weaker than those of the zwitterion. This behaviour was already observed by Gómez-Zavaglia and Fausto[26] and it has been confirmed in our experiments, although at quite different oven temperatures. The explanation given by those authors is based on local heating effects. When hot glycine molecules hit the cold substrate their thermal energy can be used to induce proton transfer and thus convert the neutral species into the zwitterionic one, more stable in the solid phase. The higher the vapour temperature, the higher the induced local heating and, hence, a more efficient conversion from neutral to zwitterions is observed.

To complement this study, we represent in Fig. 2b spectra recorded at increasing substrate temperatures of a sample generated at T_{oven} = 105 °C and deposited at T_{subs} = 25 K, and subsequently warmed at 5 K min^{-1}. The weakening of the main neutral glycine bands with growing temperature reveals the transformation of the neutral to the zwitterionic species. At 200 K the neutral species bands cannot be appreciated any more in the spectra. The spectrum at this temperature is shown in reference to a theoretical prediction later on in this work (see Fig. 4). If the sample is cooled back to 25 K the IR bands do not change appreciably.

The main parameters obtained from our DFT calculation of the zwitterionic α-glycine crystal are shown in Table 1, together with the experimental values measured by neutron diffraction,[41] used as initial geometry in the optimization processes. A representation of the unit cell is shown in Fig. 3. As we mentioned above, dispersion corrections were necessary to improve the estimation of the cell parameters and H-bond distances, with the result that the calculated parameters are in acceptable agreement with the experimental measurements. In spite of these corrections, an expansion of the unit cell volume is obtained, particularly along the b-axis on which dispersive forces have a more relevant contribution. The calculations also predict ~0.04 Å shorter H-bond distances than those obtained by neutron powder diffraction. The theoretical results imply a greater proton transfer from the ammonium group to the O atom of a carboxyl group of a neighbouring molecule. These discrepancies in the evaluation of the dispersion forces and H-bonds are normally found in DFT methods (see for example ref. 42). Overall, for those parameters not involved in H-bonding, our predicted intramolecular values are in good agreement with those experimentally obtained.

Based on the optimized structure, we have predicted the IR spectrum of the crystal, displayed in Fig. 4, and summarized in Table 2. As far as we know this is the first time that a calculated infrared spectrum of solid glycine is reported. The lower panel of the figure reproduces the experimental spectrum

Table 1 Calculated (this work) and experimental lattice parameters (a, b, c in Å, β in degrees, and volume in Å^3) and bond distances (Å) of the α-glycine crystal

Parameter	Theoretical[a]	Experimental[b]
a	5.128	5.105
b	13.066	11.969
c	5.481	5.465
β	113.065	111.697
Volume	337.88	310.25
r(N–H)	1.059	1.037
r(N–H)	1.070	1.054
r(N–H)	1.043	1.025
r(N–C)	1.490	1.476
r(C–H)	1.098	1.090
r(C–H)	1.093	1.089
r(C–C)	1.531	1.526
r(C–O)	1.271	1.250
r(C–O)	1.260	1.251
r(NH···O)$_{shortest}$	1.688	1.728

[a] PBE gradient-corrected functional (GGA), with dispersion corrections in TS scheme. [b] Ref. 41.
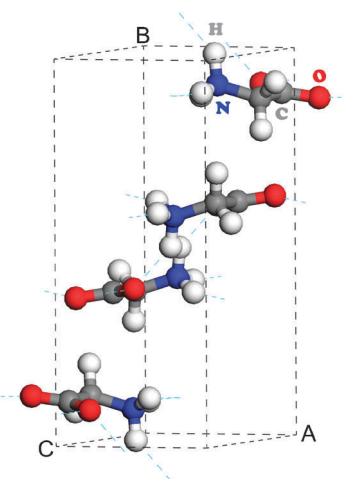

Fig. 3 Representation of the monoclinic unit cell of the calculated α-glycine crystal.

of a pure glycine film obtained by deposition at 25 K and annealed to 200 K. The comparison between the spectra is not straightforward, as the calculations do not provide information on bandwidths, an essential component in the appearance of any spectrum. Even so, the correspondence of the main absorptions between experiment and theory is clear, and the agreement could be made more evident on the overall relative intensities if the calculated bands were conveniently broadened. The deviations on the assigned vibrations collected in Table 2 are usually smaller than 5%. We have not been able to find literature values for experimental IR band strengths of glycine. Thus, although the calculated intensities could have large uncertainties, we have used these values to estimate the number of glycine molecules in our deposits.

Solid glycine in different environments

We have generated mixed solid layers of glycine/H_2O, glycine/CO_2 and glycine/CH_4 at 25 K with approximately 0.5% in mass glycine concentration. Fig. 5 displays the spectra of these
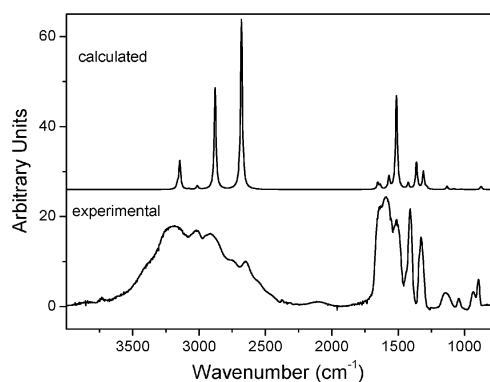
Fig. 4 IR calculated spectrum, as described in the Computational methods section, of solid crystalline α-glycine (top) compared with a pure glycine ice film obtained by deposition at 25 K followed by heating at 200 K. Theoretical bands are represented by Lorentzian curves with an arbitrary half-width at half-maximum of 8 cm^{-1}.

Table 2 Spectral assignment of crystalline α-glycine in the zwitterionic structure^a

	Experimental		Theoretical	
Assignment	Wavenumber	Intensity	Wavenumber	Intensity
νNH_3, νCH_2	3244–2551	vs	3144, 3009, 2878, 2680	17 255
δNH_3	1661–1512	s	1653–1512	6503
δCH_2	1436	sh	1424	331
νCOO	1407	m	1361	1441
ωCH_2, ωNH_3	1326	m	1309	989
ρNH_3	1138	w	1131	178
νCN	1039	w	1078, 1022	81
ρCH_2	929	w	878	51
νCC	893	w	873	132
δCOO	671	w	676	314

^{a} Wavenumber values in cm^{-1} and theoretical intensities in km mol^{-1}. Theoretical spectra calculated as described in the Computational methods section. Intensities listed are addition of the corresponding individual values, where appropriate. Qualitative experimental intensities: vs, very strong, s, strong, sh, shoulder, m, medium, and w, weak.

diluted mixtures compared with one of the pure amino acids (top panel). In all cases the glycine sublimation conditions were kept constant (T_{oven} = 105 °C).

Polar environments

Although obscured by the strong water absorption at ∼1650 cm^{-1}, panel (b) shows that the glycine spectrum of the water mixture does not change appreciably with respect to that of its pure form. The glycine bands appear at practically the same frequencies and the fraction neutral/zwitterionic remains almost the same. Table 3 collects observed and calculated values of the vibrational modes of neutral glycine (and of its dimer, see below). Our observations agree with those of Gómez-Zavaglia and Fausto[26] for vapour deposited pure glycine films at 9 K. The spectral evidence points to the conclusion that at low temperature the glycine molecules surrounded by a water ice matrix adopt a configuration that does not differ appreciably from the one it has in vapour deposited pure films. The transformation from

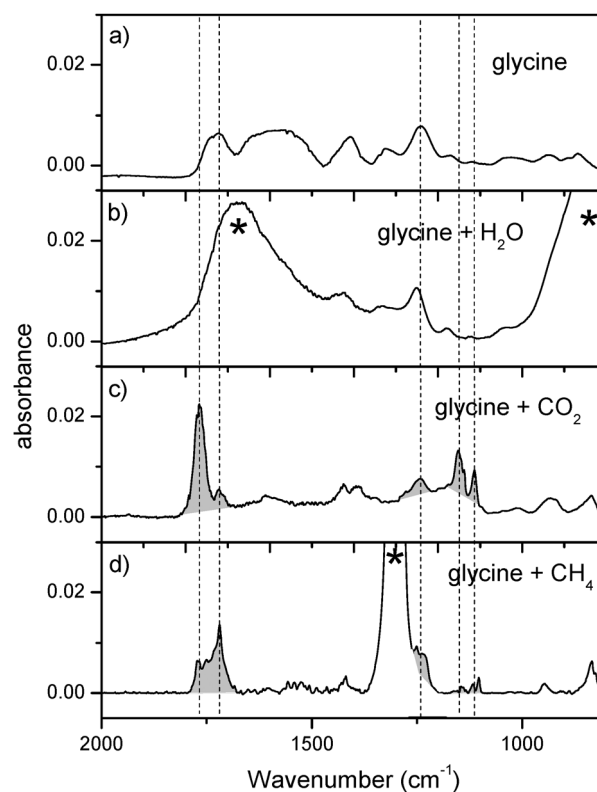**Fig. 5** Infrared spectra of solid layers generated by vapour deposition at 25 K of (a) glycine, (b) 0.5% glycine/H$_2$O, (c) 0.5% glycine/CO$_2$, (d) 0.5% glycine/CH$_4$. The asterisks (*) denote H$_2$O bands in panel (b), and a CH$_4$ band in panel (d). The shaded bands in panels (c) and (d) are discussed in the text.

neutral to zwitterionic also takes place in a similar fraction in both media. A theoretical study on neutral and zwitterionic glycine/H$_2$O complexes in Ar matrices indicates that the proton transfer between the NH$_2$ and COOH groups of glycine occurs when the amino acid is H-bonded with at least three water molecules.[43] In our co-deposited 0.5% glycine/water samples at 25 K each glycine molecule must be surrounded by more than three water molecules, and consequently the detected presence of IR absorptions associated to both forms was to be expected.

As we mentioned above, the main fingerprints of the presence of neutral glycine in our solid deposits are the bands at 1725 and 1242 cm^{-1} in the spectra of Fig. 2, listed in the second column of Table 3. The former is present in the Ar matrix spectrum[18] (column 7th of Table 3), but the second one is missing. Gómez-Zavaglia and Fausto[26] suggested that these bands could be associated to neutral glycine dimers, based on an *ab initio* calculation of the infrared spectrum of the most stable conformation in the gas phase of these dimers (a centrosymmetric structure with two equivalent H-bonds between carboxyl groups), that predicted strong absorptions around these wavenumbers. Our theoretical calculation for this dimer structure also predicted strong absorptions in these regions, as listed in the last column of Table 3. However, the relative stability of the different glycine dimer conformers is nowadays a subject of debate (see *e.g.* ref. 44–46). These studies show that different conformations could present similar stabilization energies, and therefore several conformers of the dimer having

12272 | *Phys. Chem. Chem. Phys.*, 2011, **13**, 12268–12276

This journal is © the Owner Societies 2011

Table 3 Spectra assignment of neutral glycine in different environments

Mode	Experimental						Theoretical		
	This work[a]				(Ref. 26)	(Ref. 18)	This work[b]		
	Solid	0.5% gly H$_2$O	0.5% gly CO$_2$	0.5% gly CH$_4$	Solid	Ar Matrix	Monomer (gas phase)	Monomer (in water)	Dimer
νC=O	1725	Hidden	1767, 1720	1770, 1720	1715	1779	1811 (297)	1743 (600)	1751 (701)
δNH$_2$	1650	Hidden	—	—	1643	1630	1675 (19)	1632 (46)	1676 (31)
δCH$_2$	1438	1423	1423	1420	—	1429	1457 (16)	1442 (31)	1462 (43), 1453 (56)
νC–C	1326	1326	1393	—	—	1390	1395 (12)	1395 (30)	1376 (28)
νCO + δCOH	1242	1250	1240	1240	1247	—	1305 (14)	1291 (58)	1279 (420)
τCH$_2$	1170	1175	1150	1141	1157	1130	1156 (87)	1154 (141)	1139 (42)
νCN	1117	1126	1115	1117, 1106	—	1101, 1099	1117 (222)	1112 (350)	—
τCO	1002	1041	1013	—	1010	—	—	—	1009 (152)
νCC + ωNH$_2$	934	Hidden	933	946	938	883	907 (111)	908 (141)	914 (136)
ωNH$_2$ + νCC	868	Hidden	837	833	866	801, 798	816 (89)	819 (167)	844 (321)

Ref. 26: Pure glycine vapour deposited on a cold substrate at 9 K. Ref. 18: 0.001% Glycine in an Ar matrix at 13 K. [a] Solids generated by vapour deposition on a cold substrate at 25 K. [b] Gaussian calculations for a gas phase neutral glycine molecule and dimer, and a neutral glycine monomer in PCM of water.

different infrared spectra could be present in the gas phase. Even more, in a recent paper,[45] the authors calculated several conformations of glycine dimers, including neutral, zwitterionic and even ionic species, showing that their relative stabilities depend on their environments, with the zwitterionic forms being more stable than the neutral ones in polar solutions. Consequently, the presence of dimers or aggregates of glycine in our deposits cannot be discarded, but for the assignment it must be kept in mind that different conformations could exist, with diverse infrared spectral characteristics.

On the other hand, our calculations of a neutral glycine monomer in water solution (see Table 3) predict infrared bands at 1743 and 1291 cm^{-1}, which agree nicely with those observed in the spectra. These bands become significantly more intense in solution than in the gas phase. According to this result, the presence of these bands in our spectra could simply be rationalized as arising from neutral glycine molecules in a polar environment, created either by zwitterionic glycine or water, or both.

Non-polar environments

Significant changes are noticeable in the spectra of 0.5% glycine/CO$_2$ and glycine/CH$_4$ layers (panels (c) and (d) in Fig. 5) with respect to the spectrum of the pure form (panel a). The accompanying molecules (CO$_2$, CH$_4$) are less polar than H$_2$O or glycine itself, and the conversion from neutral to zwitterionic is highly restricted. Although some zwitterionic form might be present in the glycine/CO$_2$ or glycine/CH$_4$ solid layers at 25 K, it is below the sensitivity limit of our IR spectra. We have assigned all the glycine bands observed in these mixtures to the neutral form (isolated or forming aggregates), with the assignments listed in Table 3. There are also interesting differences between the spectra in the two non-polar environments, being furthermore at variance with the spectrum recorded by Stepanian and coworkers[18] for neutral glycine in an argon matrix at 13 K. The spectral differences must reflect the diverse interactions that the glycine molecules feel in the vicinity of CO$_2$, CH$_4$ or Ar atoms in the matrix. We have

drawn broken vertical lines to emphasize the largest dissimilarities in the 800–2000 cm^{-1} mid-IR zone in Fig. 5, where the bands of interest are shaded, and for the 3400–3900 cm^{-1} O–H stretching band region in Fig. 6. The relatively narrow bands at 1150 cm^{-1} and 1115 cm^{-1}, fairly intense in the CO$_2$ mixture, are assigned to CH$_2$ twisting and CN stretching, respectively (Gómez-Zavaglia and Fausto's calculation[26] and also this work), whereas the 1240 cm^{-1} feature, much more intense in pure glycine and in glycine/H$_2$O, is ascribed to the single bond C–O stretching in coincidence with a COH bending. The intensity enhancement in the 1150 cm^{-1} band for the CO$_2$ mixture could be interpreted in terms of dipole–dipole interactions between the CH$_2$ motion and neighbouring O atoms of CO$_2$; this interaction would be much reduced for the CH$_4$ sample, where the neighbouring atoms are hydrogen atoms. The opposite would apply to the 1240 cm^{-1} C–O stretching, which would be enhanced in H-rich environments. The intensity of the double bond C=O stretch, at 1720 cm^{-1}, seems to be irregularly distributed in the non-polar samples. A very strong band appears in the CO$_2$-dominated solid at 1770 cm^{-1} accompanied by a weak feature at 1720 cm^{-1}, whereas for the CH$_4$
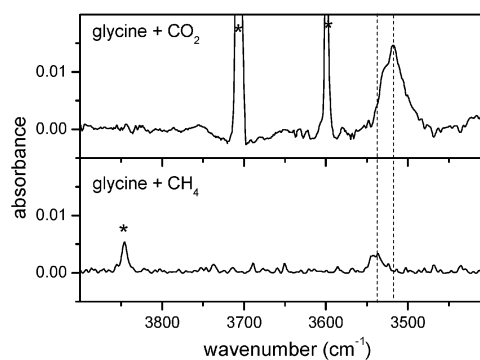

Fig. 6 Detail of the glycine OH stretching spectral region for the same two mixtures presented in panels (c) and (d) of Fig. 5. Asterisks indicate absorptions of CO$_2$ and of CH$_4$ in the top and bottom panels, respectively.

case the lower frequency peak is stronger. Without a proper knowledge of the structure of these solids, it is difficult to provide a comprehensive interpretation of these spectral features, in which the interactions between the neutral glycine with different sites of the non-polar surrounding solid must play some role.

It has also been possible to detect the OH stretching vibration of glycine trapped in these two CO_2 and CH_4 matrices (in the H_2O matrix it was buried underneath the OH stretching bands of water). This region is presented in Fig. 6. The glycine O–H absorption band appears at 3520 cm^{-1} and at 3533 cm^{-1} for CO_2 and CH_4 matrices respectively, being in the former spectrum much more intense than in the latter. This vibration is shifted to lower frequencies with respect to the experimental measurements obtained by Huisken et al.[47] for glycine trapped in Ar or Ne matrices, or in He clusters (3566 cm^{-1}, 3581 cm^{-1}, and 3585 cm^{-1} respectively). These authors observed a correlation between the frequency shift of this band and the strength of the interaction with the environment. This rule would imply in our case a stronger interaction with CO_2 or CH_4 than with the noble gas atoms of the matrices, and between CO_2 and CH_4, a slightly larger interaction (larger red shift) with the former species. This is also in agreement with the observation of this band being stronger in the CO_2 sample than in the methane counterpart, and with the parallel intensity increase in the 1150 cm^{-1} band in the CO_2 sample mentioned above.

Fig. 7 displays the temperature evolution of a pure vapour deposited glycine solid and of the three mixtures studied in this work, all with 0.5% glycine concentration. For pure glycine (top panel) at the deposition temperature (25 K), besides the predominant zwitterionic species, we have an important fraction of neutral glycine, revealed by the intensity of the already familiar two main bands associated to this species (shaded in the lowest trace of this panel). The evolution of the intensity of these two bands with temperature, extracted from the spectra shown in the four panels of Fig. 7, is displayed in panels a and b of Fig. 8. In the last panel of Fig. 8 a quantization of the fraction of the neutral species present in each deposit, obtained as was explained in the experimental part, is represented. For pure glycine and glycine/water deposits (squares and circles in Fig. 8) a slow decrease of the amount of neutral glycine as the temperature increases is observed. Interestingly, the evolution with temperature of the neutral versus zwitterionic ratio for glycine in a water ice environment is almost the same than in pure glycine, with somehow a little more neutral form in the ice water mixture. It could be expected that the polar water environment might accelerate proton transfer from the neutral to the zwitterion, but the figure indicates a similar pace in both deposits. The two pure neutral glycine bands disappear completely only at 150 K, at the same temperature when glycine is surrounded by other glycine molecules than when it is surrounded by water. At 200 K most of the water has been evaporated from the sample, and the solid zwitterionic glycine remains.

In CO_2 and CH_4 environments at 25 K all the glycine is in its neutral form. Upon heating the transformation to the zwitterionic species takes place very slowly as indicated by the reduced intensity decrease of the stretching C=O band at 1770 cm^{-1}–1720 cm^{-1} (see panel a in Fig. 8). When the solids
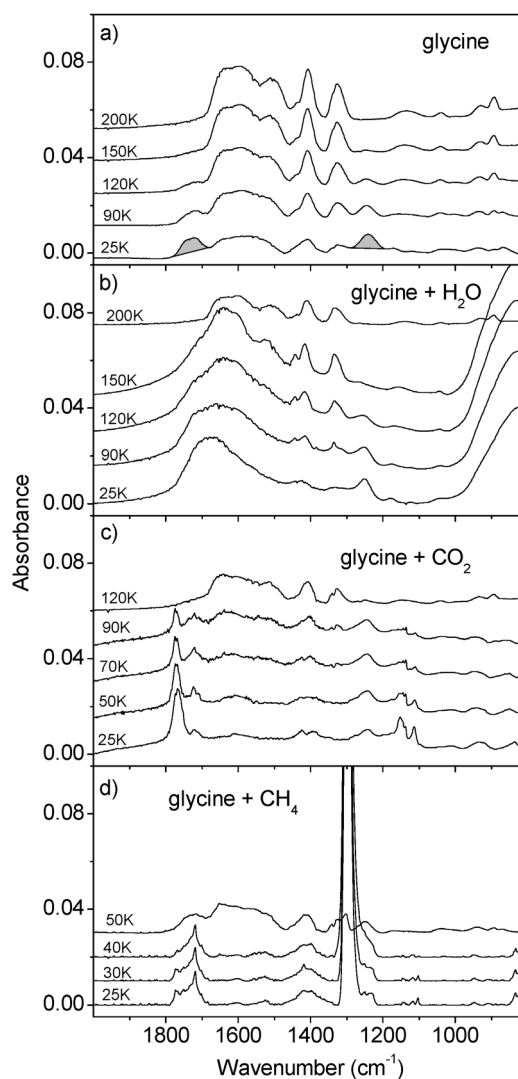

Fig. 7 Temperature evolution of IR spectra of: (a) vapour-deposited pure glycine, (b) 0.5% glycine/H_2O, (c) 0.5% glycine/CO_2, and (d) 0.5% glycine/CH_4. All samples were deposited at 25 K and heated up to sublimation of the volatile species. Spectra are offset in the absorbance scale for clarity.

are heated above the sublimation temperature of each volatile, 120 K for CO_2 and 50 K for CH_4, most of these molecules leave the sample and a pure glycine deposit is obtained. Spectra were recorded just above the sublimation temperatures, showing appreciable changes with respect to the corresponding previous cooler spectra. Once the matrix formed by the volatile species disappears the glycine residue quickly reaches the neutral/zwitterionic ratio that corresponds to pure glycine at that temperature (see panel c in Fig. 8).

Summary and conclusions

This work extends previous knowledge on the IR spectrum of glycine, and on the transformation that this molecule can undergo from the neutral to the zwitterionic form. We generated samples of pure glycine and of diluted mixtures with water, carbon dioxide and methane, molecules that could accompany glycine in astrophysical or astronomical media.
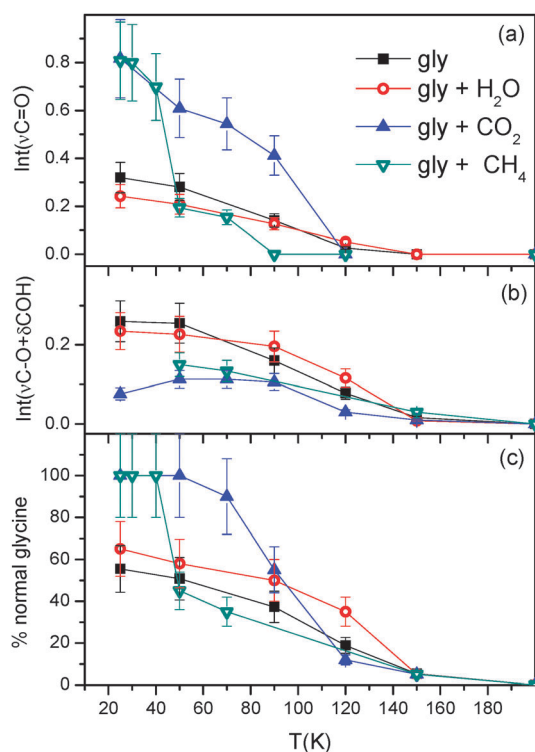
Fig. 8 Panels (a) and (b): temperature evolution of the integrated intensity of the two main IR bands associated to neutral glycine, the νC=O band at ~ 1740 cm^{-1} and the νC–O + δCOH band at ~ 1420 cm^{-1}, respectively, obtained from the spectra represented in Fig. 7. Panel (c): temperature evolution of the fraction of neutral glycine present in the samples shown in Fig. 7.

Glycine was evaporated in an oven, and the vapour was deposited, together with the other species, on a substrate kept at 25 K in a low-pressure chamber. The substrate was heated to various temperatures to study the evolution of the substances in the sample using *in situ* IR spectroscopy. Besides, theoretical calculations were performed on crystalline glycine and on molecular glycine, both isolated and surrounded by water. The main conclusions of this investigation are the following.

Vapour-deposited glycine contains a fraction of neutral glycine that depends on the generation conditions, namely temperature of the oven and of the substrate. Upon heating the neutral form transforms completely to the zwitterionic structure, which is in good agreement with previous observations of room temperature vapour deposited amino acids.[15,26] The evolution is easily followed by the changes undergone by two IR bands, assigned to the neutral species. This process had been studied before for a 9 K substrate.[26] Our results, for a 25 K substrate, cover a larger range of oven temperatures, and agree with those previously reported.

Diluted mixtures of glycine with water, on one side, and with CO_2 and CH_4, on the other, show dissimilar characteristics regarding the neutral to zwitterion transformation. In a polar environment (H_2O), glycine behaves basically in a similar manner as the pure glycine compound: the neutral content depends on the substrate temperature, decreases with increasing temperature, and is practically null at 150 K. Thus, water or zwitterionic glycine seems to have a similar effect on the neutral glycine molecules in their vicinity, favouring proton transfer to generate the ionic species.

On the other hand, glycine appears only in its neutral form at 25 K in non-polar surroundings, where the conversion to the zwitterionic structure is highly restricted. As the substrate temperature is raised, the process proceeds very slowly. At the sublimation temperature of the non-polar volatile species the transformation takes place very quickly, and the glycine remains present a very similar pattern to that of pure glycine.

Differences in the spectra recorded at 25 K for the four systems studied here (pure glycine and three mixtures) are rationalized in terms of dipole interactions between the assigned internal motions for the selected fingerprint vibrations, and the surrounding species. The analysis of the OH stretching region for the non-polar species indicates a larger interaction between glycine and CO_2 than with CH_4, and in both cases, stronger interactions than those observed with noble gas matrices too.

A solid state DFT calculation of α-glycine yields an optimized structure in reasonable agreement with the neutron diffraction measurements, especially when dispersion corrections are taken into account. The prediction of the IR spectrum of the solid is also in sound concord with the experimental observation. Theoretical calculations at a moderate level, of the individual molecule, the glycine dimer, and the molecule in a water environment offer valuable information that helps in the assignment of the spectra.

From the astrophysical point of view, the main conclusion concerns the possible structure that glycine could have in different media. It seems reasonable to suspect the presence of carbon dioxide and probably methane, besides water, accompanying glycine wherever this species could be found. As mentioned above, these non-polar species favour the neutral form of glycine, and then the most adequate spectral feature to search would be the 1750 cm^{-1} (5.71 μm) band. On the other hand, for warmer samples, or material that has undergone warming above the sublimation temperature of those gases, most glycine would be in its zwitterionic form, and the features to look for should be the 1326 cm^{-1} and 1423 cm^{-1} (7.54 μm and 7.03 μm, respectively) bands, where overlap with the water bending vibration (6.06 μm) would be small.

Acknowledgements

References

1 J. Oró, *Nature*, 1961, **190**, 389.
2 J. R. Cronin and S. Pizzarello, *Adv. Space Res.*, 1983, **3**, 5.
3 S. B. Charnley, *et al.*, *Adv. Space Res.*, 2002, **30**(6), 1419.
4 D. Brownlee, *et al.*, *Science*, 2006, **314**, 1711.

5 S. A. Sandford, *et al.*, *Science*, 2006, **314**, 1720.
6 J. E. Elsila, D. P. Glavin and J. P. Dworkin, *et al.*, *Meteorit. Planet. Sci.*, 2009, **44**, 1323.
7 M. Callahan, A. Aubrey, J. L. Bada, J. P. Dworkin, J. E. Elsila, D. P. Glavin, E. Parker and P. Jenniskens, American Astronomical Society, DPS meeting #41, #9.09, 09/2009.
8 R. B. Hoover, *J. Cosmol*, 2011, **13**, 3811–3848.
9 G. M. Muñoz Caro, U. J. Meierhenrich and W. A. Schutte, *et al.*, *Nature*, 2002, **416**, 403.
10 M. P. Bernstein, J. P. Dworkin, S. A. Sandford, G. W. Cooper and L. J. Allamandola, *Nature*, 2002, **416**, 401.
11 P. D. Holtom, C. J. Bennett, Y. Osamura, N. J. Mason and R. I. Kaiser, *Astrophys. J.*, 2005, **626**, 940.
12 C.-W. Lee, J.-K. Kim, E.-S. Moon, Y. C. Minh and H. Kang, *Astrophys. J.*, 2009, **697**, 428.
13 J.-B. Bossa, F. Duvernay, P. Theulé, F. Bogert, L. d'Hendecourt and T. Chiavassa, *Astron. Astrophys.*, 2009, **508**(2), 601.
14 M. Nuevo, G. Auger, D. Blanot and L. d'Hendecourt, *Origins Life Evol. Biosphere*, 2008, **38**, 37.
15 U. J. Meierhenrich, J. J. Filippi, C. Meinert, J. B. Bredehöft, J. Takahashi, L. Nahon, N. C. Jones and S. V. Hoffmann, *Angew. Chem., Int. Ed.*, 2010, **49**, 7799.
16 F. Duvernay, V. Dufauret, G. Danger, P. Theulé, F. Borget and T. Chiavassa, *Astron. Astrophys.*, 2010, **523**, A79.
17 A. Peeters, C. Van Alsenoy, A. T. H. Lenstra and H. J. Geise, *J. Chem. Phys.*, 1995, **103**(15), 6608.
18 S. G. Stepanian, I. D. Reva, E. D. Radchenko, M. T. S. Rosado, M. L. T. S. Duarte, R. Fausto and L. Adamowicz, *J. Phys. Chem.*, 1998, **102**, 1041.
19 C. Espinoza, J. Szczepanski, M. Vala and N. C. Polfer, *J. Phys. Chem. A*, 2010, **114**, 5919.
20 L. F. Pacios, O. Gálvez and P. C. Gómez, *J. Phys. Chem. A*, 2001, **105**, 5232.
21 M. T. Rosado, M. L. T. S. Duarte and R. Fausto, *Vib. Spectrosc.*, 1998, **16**, 35.
22 R. Ramaekers, J. Pajak, B. Lambie and G. Maes, *J. Chem. Phys.*, 2004, **120**(9), 4182.
23 G. Tzvetkov, M. G. Ramsey and F. P. Netzer, *J. Chem. Phys.*, 2005, **122**, 114712.
24 M. M. Thiam and M. Ebrahimi, *e-J. Surf. Sci. Nanotechnol.*, 2009, **7**, 693.
25 S. Gnanasambandam, Z. Hu, J. Jiang and R. Rajagopalan, *J. Phys. Chem. B*, 2009, **113**, 752.
26 A. Gómez-Zavaglia and R. Fausto, *Phys. Chem. Chem. Phys.*, 2003, **5**, 3154.
27 B. Maté, A. Medialdea, M. A. Moreno, R. Escribano and V. J. Herrero, *J. Phys. Chem. B*, 2003, **107**(40), 11098.
28 O. Gálvez, B. Maté, V. J. Herrero and R. Escribano, *Icarus*, 2008, **197**, 599.
29 R. M. Mastrapa, S. A. Shandford, T. L. Roush, D. P. Cruikshank and C. M. D. Ore, *Astrophys. J.*, 2009, **701**, 1347.
30 P. A. Gerakines, W. A. Schutte, J. M. Greenberg and E. F. van Dishoeck, *Astron. Astrophys.*, 1995, **296**, 810.
31 D. M. Hudgins, S. A. Sandford, L. J. Allamandola and G. G. M. Tielens, *Astrophys. J. Suppl.*, 1993, **86**, 713.
32 V. J. Herrero, O. Gálvez, B. Mate and R. Escribano, *Phys. Chem. Chem. Phys.*, 2010, **12**, 3164.
33 M. D. Segall, P. J. D. Lindan, M. J. Probert, C. J. Pickard, P. J. Hasnip, S. J. Clark and M. C. Payne, *J. Phys.: Condens. Matter*, 2002, **14**, 2717.
34 J. P. Perdew, K. Burke and M. Ernzerhof, *Phys. Rev. Lett.*, 1996, **77**, 3865.
35 J. P. Perdew, J. A. Chevary, S. H. Vosko, K. A. Jackson, M. R. Pederson, D. J. Singh and C. Fiolhais, *Phys. Rev. B: Condens. Matter*, 1992, **46**, 6671.
36 C. Adamo and V. Barony, *J. Chem. Phys.*, 1998, **110**, 6158.
37 A. D. Becke, *J. Chem. Phys.*, 1993, **98**, 5648.
38 A. Tkatchenko and M. Scheffler, *Phys. Rev. Lett.*, 2009, **102**, 73005.
39 S. Grimme, *J. Comput. Chem.*, 2006, **27**, 1787.
40 M. J. Frisch, G. W. Trucks, H. B. Schlegel, G. E. Scuseria, M. A. Robb, J. R. Cheeseman, J. A. Montgomery Jr, T. Vreven, K. N. Kudin, J. C. Burant, J. M. Millam, S. S. Iyengar, J. Tomasi, V. Barone, B. Mennucci, M. Cossi, G. Scalmani, N. Rega, G. A. Petersson, H. Nakatsuji, M. Hada, M. Ehara, K. Toyota, R. Fukuda, J. Hasegawa, M. Ishida, T. Nakajima, Y. Honda, O. Kitao, H. Nakai, M. Klene, X. Li, J. E. Knox, H. P. Hratchian, J. B. Cross, V. Bakken, C. Adamo, J. Jaramillo, R. Gomperts, R. E. Stratmann, O. Yazyev, A. J. Austin, R. Cammi, C. Pomelli, J. W. Ochterski, P. Y. Ayala, K. Morokuma, G. A. Voth, P. Salvador, J. J. Dannenberg, V. G. Zakrzewski, S. Dapprich, A. D. Daniels, M. C. Strain, O. Farkas, D. K. Malick, A. D. Rabuck, K. Raghavachari, J. B. Foresman, J. V. Ortiz, Q. Cui, A. G. Baboul, S. Clifford, J. Cioslowski, B. B. Stefanov, G. Liu, A. Liashenko, P. Piskorz, I. Komaromi, R. L. Martin, D. J. Fox, T. Keith, M. A. Al-Laham, C. Y. Peng, A. Nanayakkara, M. Challacombe, P. M. W. Gill, B. Johnson, W. Chen, M. W. Wong, C. Gonzalez and J. A. Pople, *Gaussian 03*, Gaussian Inc., Wallingford, CT, 2004.
41 P.-G. Jönsson and Å. Kvick, *Acta Crystallogr., Sect. B: Struct. Crystallogr. Cryst. Chem.*, 1972, **28**, 1827.
42 O. Gálvez, B. Maté, B. Martín-Llorente, V. J. Herrero and R. Escribano, *J. Phys. Chem. A*, 2009, **113**, 3321.
43 R. Ramaekers, J. Pajak, B. Lambie and G. Maes, *J. Chem. Phys.*, 2004, **120**(9), 4182.
44 J. Chocholousova, J. Vacek, F. Huisken, O. Werhahn and P. Hobza, *J. Phys. Chem. A*, 2002, **106**, 11540.
45 M. F. de Carvalho, R. A. Mosquera and R. Rivelino, *Chem. Phys. Lett.*, 2007, **445**, 117.
46 P. Friant-Michel and M. F. Ruiz-Lopez, *ChemPhysChem*, 2010, **11**, 3499.
47 F. Huisken, O. Werhahn, A. Y. Ivanov and S. A. Krasnokutski, *J. Chem. Phys.*, 1999, **111**(7), 2978.